

The crystal structure of MreC provides insights into polymer formation

Qin Xu^{1,2,3}, Ning Sun^{1,4}, Qingjie Xiao³, Chia-ying Huang⁵, Mengxue Xu^{1,4}, Weizhe Zhang³, Lina Li^{1,3}, Qisheng Wang^{1,3}, Vincent Olieric⁵, Weiwu Wang⁴, Jianhua He¹ and Bo Sun^{1,3} 

1 Shanghai Institute of Applied Physics, Chinese Academy of Sciences, Shanghai, China

2 University of Chinese Academy of Sciences, Beijing, China

3 Shanghai Advanced Research Institute, Chinese Academy of Sciences, Shanghai, China

4 Department of Microbiology, College of Life Sciences, Nanjing Agricultural University, China

5 Swiss Light Source, Paul Scherrer Institute, Villigen-PSI, Switzerland

Keywords

cell shape-determining protein; crystal structure; filament-like structure; MreC; polymer formation

Correspondence

W. Wang, Department of Microbiology, College of Life Sciences, Nanjing Agricultural University, Nanjing 210095, China

E-mail: wwwwang@njau.edu.cn

and

J. He and B. Sun, Shanghai Institute of Applied Physics, Chinese Academy of Sciences, Shanghai 201800, China

E-mails: hejianhua@sinap.ac.cn (JH) and

sunb@sari.ac.cn (BS)

Qin Xu and Ning Sun contributed equally to this article

(Received 20 August 2021, revised 1 September 2021, accepted 10 September 2021)

doi:10.1002/2211-5463.13296

MreC is a scaffold protein required for cell shape determination through interactions with proteins related to cell wall synthesis. Here, we determined the crystal structure of the major periplasmic part of MreC from *Escherichia coli* at 2.1 Å resolution. The periplasmic part of MreC contains a coiled-coil domain and two six-stranded barrel domains. The coiled-coil domain is essential for dimer formation, and the two monomers are prone to relative motion that is related to the small interface of β-barrel domains. In addition, MreC forms an antiparallel filament-like structure along the coiled-coil direction, which is different from the helical array structure in *Pseudomonas aeruginosa*. Our structure deepens our understanding of polymer formation of MreC.

Peptidoglycan, an important component of most bacterial cell walls, plays an important role in maintaining the shape of bacteria and resisting osmotic pressure [1]. Peptidoglycan is a multilayer network structure that is composed of glycan strands that are crosslinked by short peptides. The glycan strands are made by polymerization of *N*-acetyl-glucosamine and

N-acetylmuramic acid [2]. Peptidoglycan synthesis is under strict spatial and temporal control to ensure the normal growth and division of bacteria. Many antibiotics inhibit the growth of bacteria by disturbing the process of peptidoglycan synthesis [3,4].

Several enzymes are directly involved in the synthesis of peptidoglycan. Glycosyltransferases catalyze the

Abbreviations

MD, molecular dynamics simulation; PBP, penicillin-binding protein; PDB, Protein Data Bank; SEC-MALS, size exclusion chromatography with multiangle light scattering detection.

polymerization of the polysaccharide chain. Transpeptidases, also called penicillin-binding proteins (PBPs), crosslink the short peptides between glycan strands [1,4]. Besides, MreB, MreC and MreD help the localization of PBPs in *E. coli* and form a complex with specific PBPs to catalyze the peptidoglycan formation [5,6]. MreB is the actin homologue that forms the cytoskeletal filaments to maintain the shape of bacterium [7,8]. The two genes of *mreC* and *mreD* are located downstream of *mreB* in the same operon [9]. These three genes code for proteins that have been shown to maintain the rod-like structure of cells, and the deletion of these genes leads to the formation of spherical cells and cell lysis in *E. coli* and *Bacillus subtilis* [5,10,11]. Previous studies have shown that MreC interacts with MreB, MreD and PBPs [5,12,13]. These proteins in *B. subtilis* have a similar trajectory around the cell [14]. Subcellular distribution of MreB in the cytoplasm depends on both MreC and MreD in *E. coli* [5]. MreC acts as a hub in complex formation. Besides, previous study also showed MreC in *Caulobacter crescentus* presents a helical or banded pattern [15]. Interestingly, MreC can maintain helical localization pattern in the periplasmic space, even when the compound A22 was used to disrupt the polymerization of MreB [15,16]. Further, internal reflection fluorescence microscopy revealed that MreB and MreC form patches that showed circumferential motion [17]. Another study revealed that MreB can form the structure of antiparallel filaments *in vivo* [7]. Considering that MreC and MreB have similar distribution characteristics, and MreC can maintain the structural characteristics after disrupting the polymerization of MreB, it is suggested that MreC may also form a filament-like structure.

The crystal structure of the major periplasmic part of MreC has been reported for some species [6,18]. The complex crystal structure of MreC and PBP2 has also been determined for *Helicobacter pylori* and showed that MreC acts as a scaffold protein to regulate the synthesis of peptidoglycan [13]. Here, we determined the crystal structure of the major periplasmic domain of MreC from *E. coli* at 2.1 Å resolution, revealing an antiparallel filament-like state that has not been reported yet.

Materials and methods

Expression and purification

The cDNA of encoding periplasmic part MreC (position of amino acid: 36–367) from *E. coli* BL21(DE3) strain was subcloned into Pet21b. *E. coli* BL21(DE3) cells carrying the

MreC expression plasmid grow in LB medium at 37 °C, and MreC overexpression was induced by adding 0.4 mM isopropyl- β -thiogalactoside when absorbance (A_{600}) reached between 0.6 and 0.8. The cells were further grown overnight at 22 °C and harvested by centrifugation. Cells were homogenized in lysis buffer [25 mM Tris–HCl (pH 8.0), 150 mM NaCl and 1 mM PMSF] and lysed using cell disruptor. The bacteria lysate was centrifuged at 13,800 g for 1 h. The supernatant was then loaded to equilibrated nickel-nitrilotriacetic acid chromatography (Ni-NTA, Qiagen, Germantown, MD, USA) resin twice. The resin was washed with wash buffer [25 mM Tris–HCl (pH 8.0), 150 mM NaCl, 20 mM imidazole]. The purpose protein was eluted with a solution of 25 mM Tris–HCl (pH 8.0), 150 mM NaCl and 300 mM imidazole. Eluted protein was then concentrated for further purification by gel filtration Superdex 200 Increase 10/300 GL column in 25 mM Tris–HCl (pH 8.0), 150 mM NaCl. The peak fractions were collected and snap frozen in liquid nitrogen and stored at –80 °C for crystallization.

MreC was crystallized at 18 °C using the sitting-drop vapor diffusion method. The crystals appear in about 2 weeks, and the crystallization condition consisted of 9.9% Isopropanol, 9.9% (v/v) polyethylene glycol (PEG3350) and 0.1 M Tris–HCl (pH 8.5). All crystals were harvested and immediately snap-frozen in liquid nitrogen after soaking in cryoprotectant that contains 25% glycerol.

Data collection and structure determination

The datasets of MreC were collected at beamlines BL18U1 and processed with HKL3000 [19,20]. The structure of MreC was solved by molecular replacement using Phaser [21] and MreC from *Listeria monocytogenes* Protein Data Bank (PDB: 2J5U) as the initial model. Major periplasmic domain of the protein shares 25% sequence identity with MreC of *E. coli*. The model of MreC was completed by using iterative refinement and model building by PHENIX [22,23] and Coot [24]. The refinement statistics are summarized in Table 1.

Size exclusion chromatography with multiangle light scattering detection

Size exclusion chromatography with multiangle light scattering detection (SEC-MALS) experiments were carried out at 25 °C with multiangle light scattering detector (MALS; Wyatt Dawn Heleos-II) and a size exclusion chromatography (Superdex 200 Increase 10/300 GL column) for measuring the relative molecular mass of protein. Protein samples (~ 2 mg·mL^{–1}, 100 μ L) were injected in a buffer containing 25 mM Tris–HCl (pH 8.0) and 150 mM NaCl. ASTRA software (Wyatt Technology, Santa Barbara, CA, USA) was used to calculate the molecular weight of protein.

Table 1. Data collection and refinement statistics. The value in parentheses is statistics parameter of the highest resolution shell. R_{merge} was defined by Diederichs and Karplus [29]. $CC_{1/2}$ is the Pearson correlation coefficient of two half datasets as described by Karplus and Diederichs [30]. SSRF, Shanghai Synchrotron Radiation Facility.

Data	MreC
Integration package	HKL3000
Beamlines of SSRF	BL18U1
Space group	C_121
Unit cell (Å)	133.3 47.6 77.3
Unit cell (°)	90 99.2 90
Wavelength (Å)	0.9793
Resolution (Å)	29.85 to 2.1 (2.14 to 2.1)
R_{merge} (%)	0.104 (0.474)
$CC_{1/2}$	0.99 (0.70)
I/σ	7.1 (1.3)
Completeness (%)	98.9 (94.0)
No. of measured reflections	83 679 (3403)
No. of unique reflections	27 880 (1309)
Redundancy	3
$R_{\text{work}}/R_{\text{free}}$ (%)	18.7/23.6
No. of atoms	3471
Protein	3285
Others	186
Average B value (Å ²)	38.5
Protein	38.6
Others	37.7
rmsd	
Bonds (Å)	0.0059
Angle (°)	0.83
Ramachandran plot statistics (%)	
Most favorable	96.68
Allowed	3.32
Disallowed	0

Molecular dynamics simulation

Molecular dynamics simulations (MDs) were carried using GROMACS software with CHARMM36 force field (<http://www.gromacs.org/>) [25]. With periodic boundary conditions, the simulation was conducted in a cubic box with a dimension of $150 \times 150 \times 150 \text{ \AA}^3$. The minimum distance was set to 2.5 nm between the protein and edge of the box. The system was solvated with TIP3P for the water model and added with 150 mM NaCl. To relax the original structure, we used the steepest descent minimization method. After 12.5 ps NVT (constant number of particles, volume and temperature) and 125 ps NPT (constant number of particles, pressure and temperature) equilibrations, we positioned the restraints of the protein. The simulation was further run for 100 ns with 2-fs timestep at temperature of 310 K and constant pressure (1 bar). During the MD process, the bond length was constrained by the LINCS algorithm [26]. The electrostatic interactions were calculated using the Particle Mesh Ewald method, with a cutoff of 10 Å for nonbonded interactions [27].

Results

Overall structure of MreC periplasmic domain

The full-length MreC in *E. coli* contains a predicted transmembrane helix and periplasmic domain. The periplasmic domain is divided into a coiled coil, a β -barrels domain and a pro-rich region (Fig. 1A). We purified the truncated MreC (residues 36–367), which lacks the N-terminal transmembrane region. The crystal of MreC diffracted to 2.1 Å resolution with space group $C121$ and unit cell $a = 133.3 \text{ \AA}$, $b = 47.6 \text{ \AA}$, $c = 77.3 \text{ \AA}$, $\alpha = \gamma = 90^\circ$ and $\beta = 99.2^\circ$ (Table 1). The overall crystal structure shows a dimeric state of the periplasmic part of MreC in the asymmetric unit (Fig. 1B). Each monomer contains a long N-terminal coil and two six-stranded barrels. Two N-terminal coils interweave with each other, and the coil of one copy inserts into the position between C-terminal β -barrels and the N-terminal coil of another copy. The area of interface between the two monomers is 2214.3 \AA^2 . The area of interface for coiled coil and the other monomer is 1994.2 \AA^2 , while the area of the interface between the β -barrel domain of the two monomers is only 306.2 \AA^2 . This implies that the interface between β -barrels of the two monomers is weak, and the coiled coil is important for maintaining the dimer structure. The molecular weight of the truncated MreC is about 37 kDa, while the result of SEC-MALS indicated a molecular weight of about 73 kDa (Fig. 1C). These results suggested that MreC exists as a dimer in solution, which is consistent with the crystal structure (Fig. 1B).

Further analysis of the details of the interfaces showed that pairs of leucine establish a leucine zipper that maintains the interaction for two coiled coils (Fig. 2A). The pairs of leucine residues include Leu80, Leu84, Leu91, Leu94, Leu104 and Leu108. Besides, some polar residues provide hydrogen bond interactions (Fig. 2A). The residues of interaction for the coiled coils were listed in Fig. 2B. These residues are relatively conserved in bacteria (Fig. 2C), although MreC in different species has a lower sequence identity. We suggest that MreC in other species also forms a dimer by coiled-coil interaction.

Structure superposition of MreC from different species

Five structures of periplasmic MreC have been solved. MreC from *L. monocytogenes* contains the N-terminal coiled coil, which forms an asymmetric dimer. Another two structures contain only the β -barrels domain with

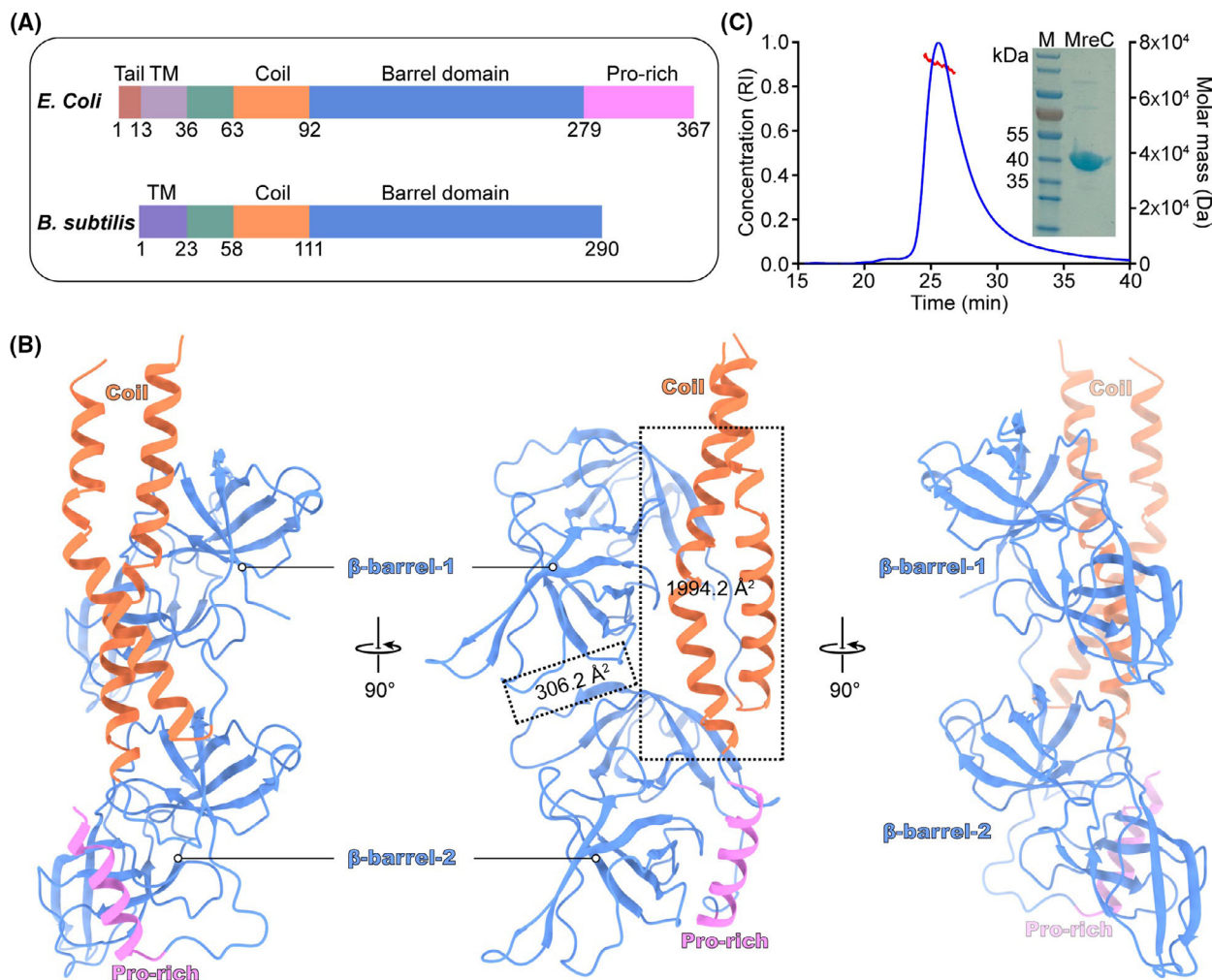


Fig. 1. Crystal structure of MreC from *E. coli*. (A) Domain arrangement of MreC. (B) Overall structure of periplasmic domain for MreC in an asymmetric unit. The interaction interface was calculated via PDBePISA. (C) SEC-MALS experiments. The calculated molar masses are indicated by the red line. Lane 1, protein marker; lane 2, purified MreC. Pro-rich, compositional bias for proline; RI, refractive index; TM, transmembrane helix.

$C\alpha$ rmsd of 0.897 Å (*E. coli*/*L. monocytogenes*), 1.743 Å (*E. coli*/*S. pneumoniae*) and 5.13 Å (*E. coli*/*H. pylori*), respectively (Fig. 3A). Further, we compared the relative positions of the two monomers by superposing the β -barrels domain of chain A for *E. coli*, *L. monocytogenes* and *H. pylori* (Fig. 3B,C). The packing of the two monomers is similar, but there is a deflection of about 30° for the coiled coil and about 10 Å movement for the β -barrel domains between *E. coli* and *L. monocytogenes* (Fig. 3D). There is a movement of about 15 Å for the β -barrel domains between *E. coli* and *H. pylori* (Fig. 3D). The interface between the β -barrels of the two monomers is weak, which may suggest that the domains are easy to move relatively to each other. Further, MD was carried out

for 100 ns to investigate the change for relative positions of the two monomers (Fig. 4A). The rmsd of $C\alpha$ for the overall structure is about 4 Å in 100 ns. Interestingly, the rmsd of $C\alpha$ is <1.5 Å for barrel domain of the two monomers (Fig. 4A), which suggest the barrel domain is relatively rigid. Snapshots captured from different times intuitively showed the obvious movement between the two monomers (Fig. 4B–D).

Filament-like form of MreC in the crystal

MreC solved from this study forms antiparallel double-filaments-like structure of head to tail in the crystal after generating the symmetry mate (Fig. 5A). The interaction for two adjacent filaments was formed

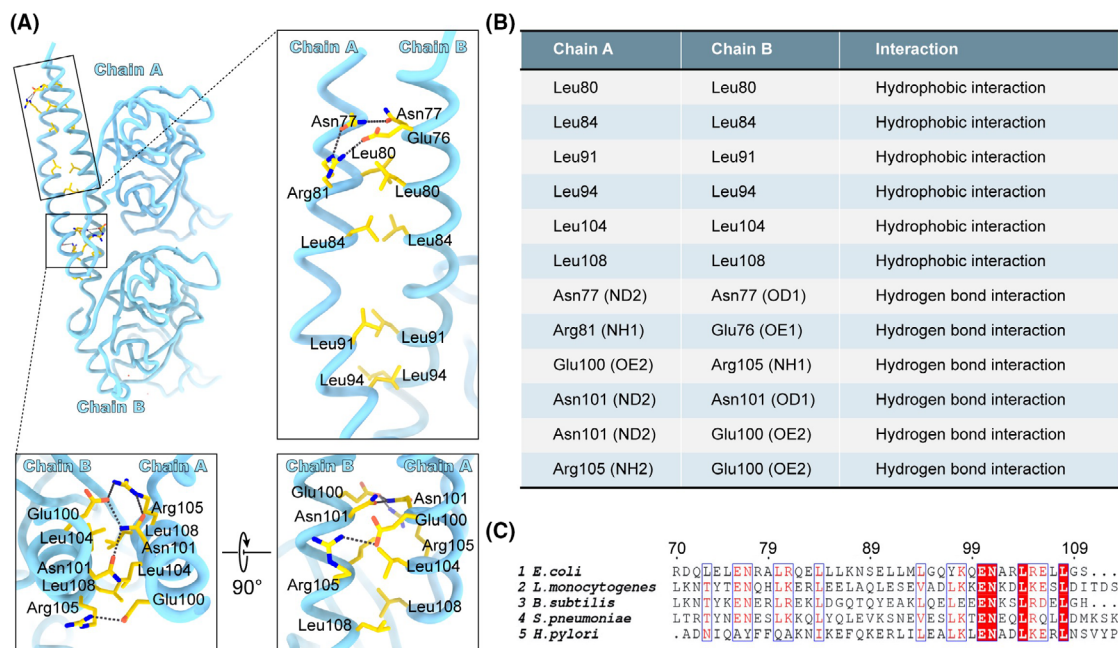


Fig. 2. Interaction of coiled coil. (A) Residues that are involved in interaction are shown as stick-and-ball model. The hydrogen bonds were shown by black dashed line. The oxygen and nitrogen atoms are colored red and blue. (B) Table listed the residues of interaction for the coiled coil between chain A and chain B. (C) Alignment of coiled-coil sequence from multiple bacteria.

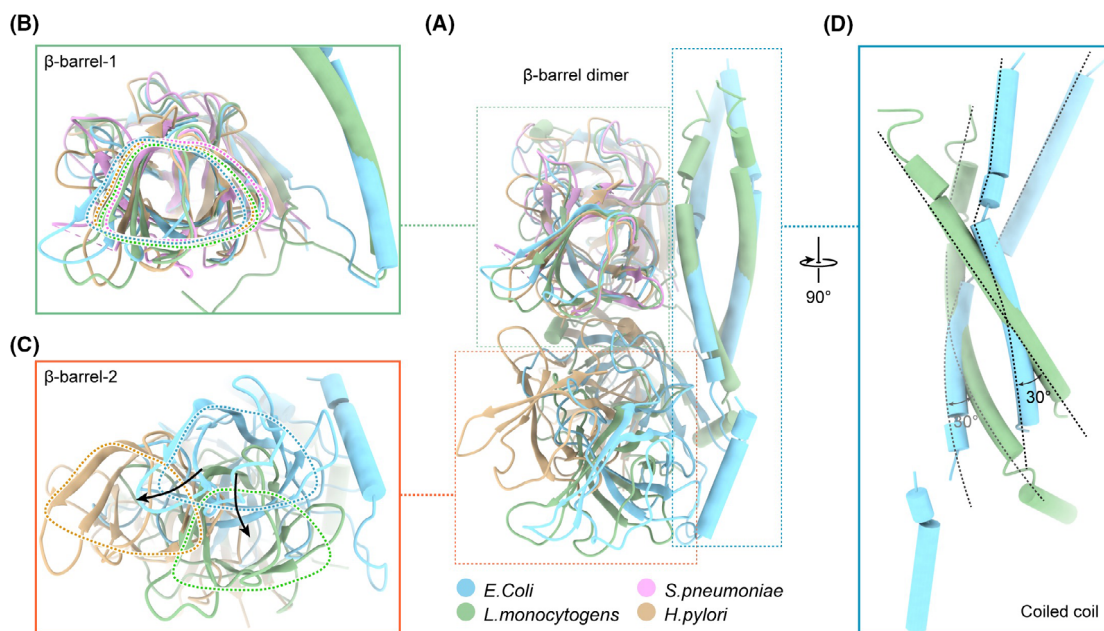


Fig. 3. Structure comparison of MreC periplasmic domain from *E. coli*, *L. monocytogenes* (PDB: 2J5U), *S. pneumoniae* (PDB: 2QF5) and *H. pylori* (PDB: 5LP5). Rectangular region is the local enlarged view. The circle corresponds to the outline of β -barrel domain. (A) Superposition of MreC periplasmic domain from *E. coli*, *L. monocytogenes* (PDB: 2J5U), *S. pneumoniae* (PDB: 2QF5) and *H. pylori* (PDB: 5LP5). Rectangular region is the local enlarged view for β -barrel-1 domain (B), β -barrel-2 domain (C) and coiled coil (D), respectively. The circle corresponds to the outline of β -barrel domain.

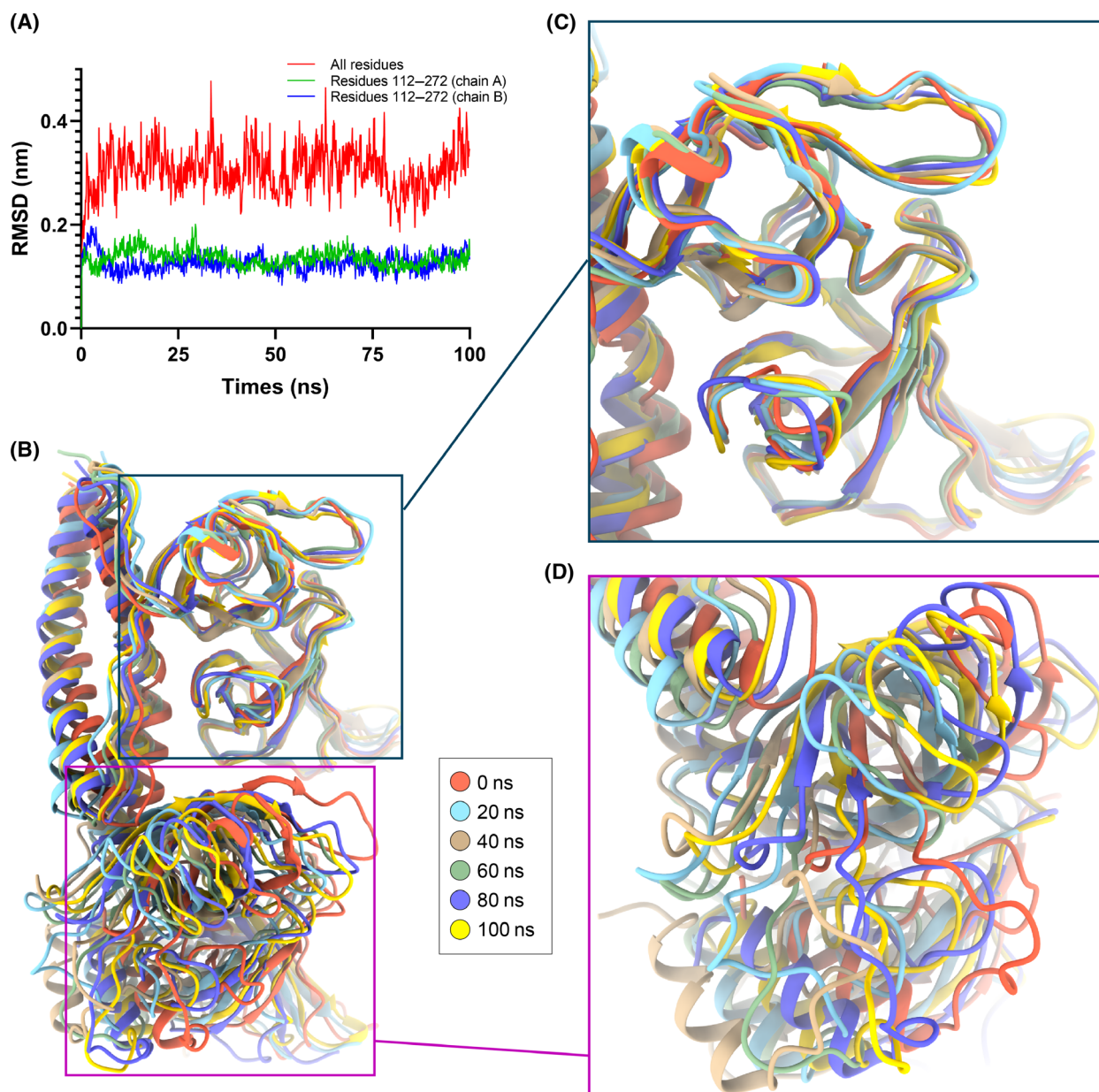


Fig. 4. MD for the crystal structure of MreC. (A) rmsd values of C α atom (with respect to the crystal structure) during 100-ns MD simulations. Red line refers to rmsd values of the overall crystal structure, and blue line and green line refer to rmsd values for β -barrels domain of A chain and B chain, respectively. (B) Snapshots are extracted every 20 ns, and β -barrels domain of A chain is overlapped to observe the position change of two monomers. Rectangular region is the local enlarged view for β -barrel domain of A chain (C) and β -barrel domain of B chain (D), respectively.

by the two barrel-shaped domains on the other side of the coil (Fig. 5A). The dimer coiled-coil interface is only 291 \AA^2 , which is unlikely to maintain the filaments-like structure on its own. The tetramer form provides a larger interface for the formation of the filament structure (Fig. 5A). The interface of junction is about 1125 \AA^2 as calculated by Proteins, Interfaces,

Structures and Assemblies (PISA). The area of the interface is relatively large compared with MreB from *Caulobacter vibrioides* that also has been reported as forming filament with 844 \AA^2 at the junction interface. Besides, another group resolved recently the structure of helical array MreC (PDB: 6ZLV) from *P. aeruginosa* by electron microscopy with the tetramer as a

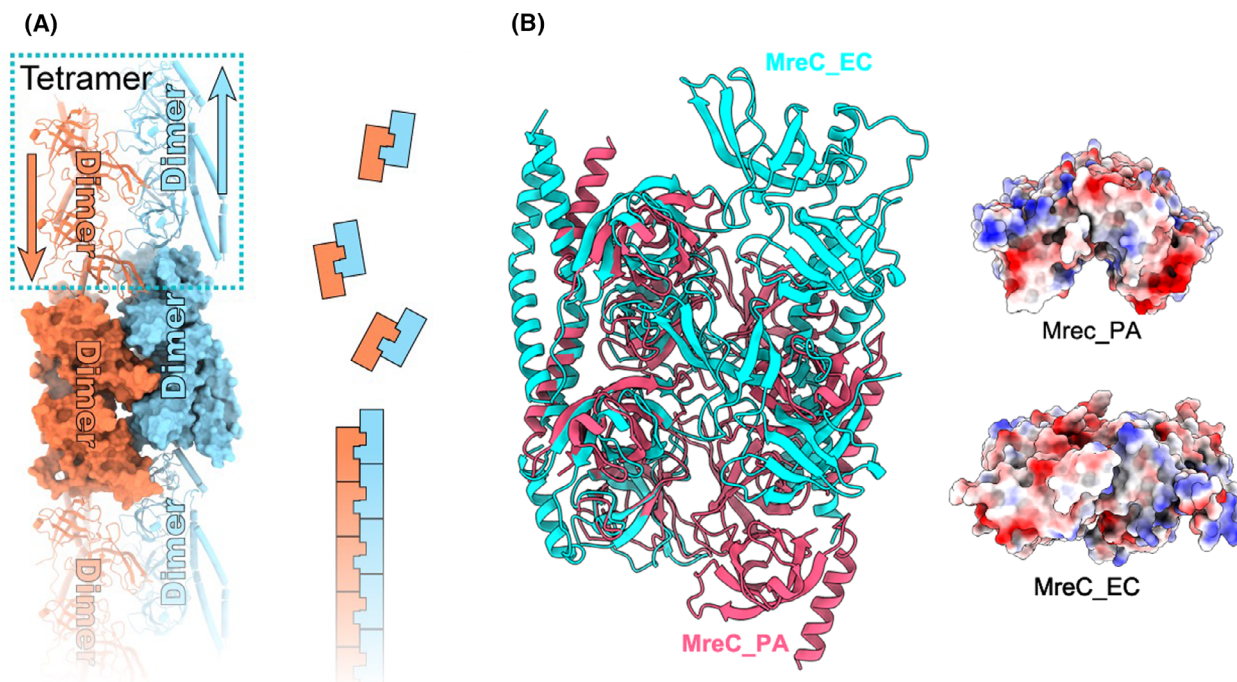


Fig. 5. MreC packing to the state of antiparallel filament-like. (A) Left is the packing of MreC with the C_{121} symmetry, and right is a model diagram for filament structure. (B) Left is a structure comparison of tetramer from *E. coli* and *P. aeruginosa*, and right is electrostatic surface potential of MreC that is viewed along the direction of coiled coil. EC, *E. coli*; PA, *P. aeruginosa*.

unit [28]. Coiled-coil and β -barrels part of MreC from *E. coli* and *P. aeruginosa* share about 42% sequence identity, and the value of rmsd is about 0.85 Å over 135 $C\alpha$ atoms of monomer and 2.8 Å over 296 $C\alpha$ atoms of dimer. The tetramer state of MreC from *E. coli* and *P. aeruginosa* is formed by the interaction of β -barrels part from two dimers with reversed orientations (Fig. 5B). Interestingly, an obvious difference is the tetramers from *P. aeruginosa* show a semicylinder associated with an angle of 135° between the two dimers, while the tetramers from *E. coli* show a plane surface (Fig. 5B).

Discussion

Previous studies have shown that MreC forms a dimer through a coiled coil [5,6]. The crystal structure reveals that the formation of the MreC dimer is related to the interaction of coiled coils, which contain a leucine repeat conserved among different species. This indicates that the MreC dimer is important to its function. Despite the local structure similarity of MreC with α -lytic protease (PDB: 1QQ4) and the serine protease (PDB: 2AS9) [18], there is no evidence that MreC has catalytic functions. More evidence showed that MreC may act as a scaffold that can interact with various proteins to affect the spatial positioning of

peptidoglycan synthesis. So far, five MreC structures from different species have been reported with sequence identity from 14% to 40% and share a similar three-dimensional structure. Comparison of multiple structures and MD provides possible insights into the structural characteristics of MreC as dynamic and adaptable. Structure comparison of different species and MD showed that the small interface between β -barrel domains is helpful to adjust the relative position of two monomers that is related to the interaction of various proteins for MreC. In turn, the coiled coil can help maintain the dimer state and stabilize the β -barrel domain array. The array is conducive to the formation of tetramer by a larger interaction interface that is provided by the barrel-like domain.

Besides, studies in vivo have suggested that MreC may form polymers, but it is not clear about this mechanism. The crystal structure of MreC in *E. coli* in this study reports the antiparallel filaments-like form that is formed by an arrangement of tetramers as a unit. A recently released MreC structure (PDB: 6ZLV) presents polymers that are a helical arrangement in a tetramer unit. Considering the obvious difference of conformation in the tetramers between MreCs from *E. coli* and *P. aeruginosa*, we speculate that tetramer conformation is related to the polymer state of the helical arrangement and filament-like. The structure

provides an understanding of the mechanism of polymers formation.

Acknowledgements

We thank the staff from beamline BL17U1, BL18U1, BL19U1, BL19U2 and the User Experiment Assist System of Shanghai Synchrotron Radiation Facility and the staff from beamline X06SA, X06DA of Swiss Light Source for on-site assistance. This work was supported by grants from the National Key R&D Program of China (2017YFA0504901) and Youth Innovation Promotion Association, Chinese Academy of Sciences (2021285).

Conflict of interest

The authors declare no conflict of interest.

Author contributions

JH, BS, QX and QX conceived and designed the experiments. QX and NS purified and crystallized protein. BS, QX, MX, WZ and LL collected the diffraction datasets and solved the structures. QX carried out MDs. JH, WW and BS wrote the manuscript. VO, CH and QW modified the paper. BS, JH and WW supervised the research.

Data accessibility

The structure factors and atomic coordinates of the MreC crystal structure are deposited in the PDB under accession number [7EFT](#).

References

- 1 Typas A, Banzhaf M, Gross CA and Vollmer W (2011) From the regulation of peptidoglycan synthesis to bacterial growth and morphology. *Nat Rev Microbiol* **10**, 123–136.
- 2 Holtje JV (1998) Growth of the stress-bearing and shape-maintaining murein sacculus of *Escherichia coli*. *Microbiol Mol Biol Rev* **62**, 181–203.
- 3 Macheboeuf P, Contreras-Martel C, Job V, Dideberg O and Dessen A (2006) Penicillin binding proteins: key players in bacterial cell cycle and drug resistance processes. *FEMS Microbiol Rev* **30**, 673–691.
- 4 Lovering AL, Safadi SS and Strynadka NC (2012) Structural perspective of peptidoglycan biosynthesis and assembly. *Annu Rev Biochem* **81**, 451–478.
- 5 Kruse T, Bork-Jensen J and Gerdes K (2005) The morphogenetic MreBCD proteins of *Escherichia coli* form an essential membrane-bound complex. *Mol Microbiol* **55**, 78–89.
- 6 van den Ent F, Leaver M, Bendezu F, Errington J, de Boer P and Lowe J (2006) Dimeric structure of the cell shape protein MreC and its functional implications. *Mol Microbiol* **62**, 1631–1642.
- 7 van den Ent F, Izore T, Bharat TA, Johnson CM and Lowe J (2014) Bacterial actin MreB forms antiparallel double filaments. *Elife* **3**, e02634.
- 8 Vats P, Shih YL and Rothfield L (2009) Assembly of the MreB-associated cytoskeletal ring of *Escherichia coli*. *Mol Microbiol* **72**, 170–182.
- 9 Wachi M, Doi M, Okada Y and Matsushashi M (1989) New mre genes mreC and mreD, responsible for formation of the rod shape of *Escherichia coli* cells. *J Bacteriol* **171**, 6511–6516.
- 10 Leaver M and Errington J (2005) Roles for MreC and MreD proteins in helical growth of the cylindrical cell wall in *Bacillus subtilis*. *Mol Microbiol* **57**, 1196–1209.
- 11 Bendezu FO and de Boer PA (2008) Conditional lethality, division defects, membrane involution, and endocytosis in mre and mrd shape mutants of *Escherichia coli*. *J Bacteriol* **190**, 1792–1811.
- 12 El Ghachi M, Mattei PJ, Ecobichon C, Martins A, Hoos S, Schmitt C, Colland F, Ebel C, Prévost MC, Gabel F *et al.* (2011) Characterization of the elongasome core PBP2: MreC complex of *Helicobacter pylori*. *Mol Microbiol* **82**, 68–86.
- 13 Contreras-Martel C, Martins A, Ecobichon C, Trindade DM, Mattei PJ, Hicham S, Hardouin P, Ghachi ME, Boneca IG and Dessen A (2017) Molecular architecture of the PBP2-MreC core bacterial cell wall synthesis complex. *Nat Commun* **8**, 776.
- 14 Garner EC, Bernard R, Wang W, Zhuang X, Rudner DZ and Mitchison T (2011) Coupled, circumferential motions of the cell wall synthesis machinery and MreB filaments in *B. subtilis*. *Science* **333**, 222–225.
- 15 Divakaruni AV, Loo RR, Xie Y, Loo JA and Gober JW (2005) The cell-shape protein MreC interacts with extracytoplasmic proteins including cell wall assembly complexes in *Caulobacter crescentus*. *Proc Natl Acad Sci USA* **102**, 18602–18607.
- 16 Dye NA, Pincus Z, Theriot JA, Shapiro L and Gitai Z (2005) Two independent spiral structures control cell shape in *Caulobacter*. *Proc Natl Acad Sci USA* **102**, 18608–18613.
- 17 Dominguez-Escobar J, Chastanet A, Crevenna AH, Fromion V, Wedlich-Soldner R and Carballido-Lopez R (2011) Processive movement of MreB-associated cell wall biosynthetic complexes in bacteria. *Science* **333**, 225–228.
- 18 Lovering AL and Strynadka NCJ (2007) High-resolution structure of the major periplasmic domain from the cell shape-determining filament MreC. *J Mol Biol* **372**, 1034–1044.

- 19 Otwinowski Z and Minor W (1997) Processing of X-ray diffraction data collected in oscillation mode. *Methods Enzymol* **276**, 307–326.
- 20 Qi-Sheng W, Feng Y, Sheng H, Bo S, Kun-Hao Z, Ke L, Zhi-Jun W, Chun-yan X, Si-Sheng W, Li-Feng Y *et al.* (2015) The macromolecular crystallography beamline of SSRF. *Nucl Sci Tech* **26**, 12–17.
- 21 McCoy AJ, Grosse-Kunstleve RW, Adams PD, Winn MD, Storoni LC and Read RJ (2007) Phaser crystallographic software. *J Appl Crystallogr* **40**, 658–674.
- 22 Afonine PV, Grosse-Kunstleve RW, Echols N, Headd JJ, Moriarty NW, Mustyakimov M, Terwilliger TC, Urzhumtsev A, Zwart PH and Adams PD (2012) Towards automated crystallographic structure refinement with phenix.refine. *Acta Crystallogr D* **68**, 352–367.
- 23 Adams PD, Afonine PV, Bunkóczi G, Chen VB, Davis IW, Echols N, Headd JJ, Hung LW, Kapral GJ, Grosse-Kunstleve RW *et al.* (2010) PHENIX: a comprehensive Python-based system for macromolecular structure solution. *Acta Crystallogr D* **66**, 213–221.
- 24 Emsley P and Cowtan K (2004) Coot: model-building tools for molecular graphics. *Acta Crystallogr D* **60**, 2126–2132.
- 25 Huang J and MacKerell AD Jr (2013) CHARMM36 all-atom additive protein force field: validation based on comparison to NMR data. *J Comput Chem* **34**, 2135–2145.
- 26 Hess B (2008) P-LINCS: a parallel linear constraint solver for molecular simulation. *J Chem Theory Comput* **4**, 116–122.
- 27 Harvey MJ and De Fabritiis G (2009) An implementation of the smooth particle mesh ewald method on GPU hardware. *J Chem Theory Comput* **5**, 2371–2377.
- 28 Martins A, Contreras-Martel C, Janet-Maitre M, Miyachiro MM, Estrozi LF, Trindade DM, Malospirito CC, Rodrigues-Costa F, Imbert L, Job V *et al.* (2021) Self-association of MreC as a regulatory signal in bacterial cell wall elongation. *Nat Commun* **12**, 2987.
- 29 Diederichs K and Karplus PA (1997) Improved R-factors for diffraction data analysis in macromolecular crystallography. *Nat Struct Biol* **4**, 269–275.
- 30 Karplus PA and Diederichs K (2012) Linking crystallographic model and data quality. *Science* **336**, 1030–1033.